



# Ultraviolet cavity ring-down spectroscopy of free radicals in etching plasmas

J.P. Booth<sup>\*</sup>, G. Cunge, L. Biennier, D. Romanini, A. Kachanov

*Laboratoire de Spectrométrie Physique, Université Joseph Fourier-Grenoble, BP 87, F-38402 St. Martin d'Hères, France*

Received 29 November 1999; in final form 13 December 1999

## Abstract

Many reactive species of interest in technological plasmas absorb light in the UV spectral region (200–300 nm). Measurement of these weak absorbances (typically  $10^{-2}$ – $10^{-4}$  for a single pass) allows us to determine their absolute concentration. Low-resolution absorption spectra of these systems have previously been obtained by broad-band absorption spectroscopy. Here we present spectra obtained using laser cavity ring-down spectroscopy, which has much higher spectral resolution, and potentially higher sensitivity. Spectra were obtained for CF, CF<sub>2</sub>, AlF and SiF<sub>2</sub> radicals in capacitively-coupled radio-frequency plasmas in fluorocarbon gases. This technique offers the possibility of real-time (1 s) absolute concentration measurements during wafer processing. © 2000 Elsevier Science B.V. All rights reserved.

## 1. Introduction

Small poly-atomic radicals, such as CF and CF<sub>2</sub>, play an important role in determining the etch rate, selectivity and anisotropy of industrial plasma etching processes [1–3]. Measurements of their concentrations allow one to test models of the physical chemistry of these systems. Furthermore, simple, reliable techniques for the detection of reactive intermediates are needed to optimise reactor and process development, and in the long term may be useful for in-situ process control. To date a variety of techniques have been used. Whereas laser-induced fluorescence (LIF) offers excellent signal-to-noise (S/N) ratio and spatial and temporal resolution [4–6], it only gives relative concentrations unless calibration

techniques are used [7]. Absorption techniques, in contrast, give the absolute (line-integrated) concentration directly, albeit with poorer spatial resolution and S/N ratios. Far-infrared diode laser absorption has been used to detect an impressive range of species [8–10], but sophisticated equipment is needed. The time-honoured technique of broad-band UV absorption spectroscopy, combined with the sensitive multi-channel optical detectors that are currently available, allows one to readily observe single-pass absorbances in the range  $10^{-3}$  or less. Whereas its spectral resolution (determined by the spectrograph) cannot match that of tunable lasers, it has the advantage that the whole absorption spectrum of a molecule can be recorded simultaneously. A substantial number of key species have been detected using this rather simple technique [11].

The recently developed laser technique of cavity ring-down spectroscopy (CRDS) [12,13] allows one

<sup>\*</sup> Corresponding author. Fax: +33-4-76514544; e-mail: jean-paul.booth@ujf-grenoble.fr

to detect very weak absorbances (linear absorption coefficients as low as  $10^{-10} \text{ cm}^{-1}$  [14]), and has been applied to transient species detection in plasmas in a few cases [15,16]. In this technique, a narrow-band tunable laser beam is injected into a high- $Q$  optical cavity, consisting of high-reflectivity spherical mirrors, and containing the sample to be analysed (the plasma in this case). Pulsed lasers are generally used, although recently the technique has been extended to modulated continuous lasers [17]. The injected fraction of the intense laser pulse remains trapped inside the cavity, its intensity decaying exponentially in time due to losses,  $T$ , at each reflection (which includes mirror transmission, surface and diffraction losses). The light re-transmitted outside the cavity is detected, allowing the photon lifetime in the cavity to be measured. The exponential decay lifetime,  $\tau(\lambda)$ , is monitored while the laser wavelength is tuned across each absorption line of the sample, and is related to the single-pass Napierian absorbance of the sample,  $A_c(\lambda)$ , by

$$l/c\tau(\lambda) = T + A_c(\lambda),$$

where  $c$  is the speed of light and  $l$  the cavity length. The mirror losses,  $T$ , vary only slowly with wavelength, giving a broad-band smooth base-line which can be easily distinguished from the rapidly varying spectral features of the sample. The density of the absorbing species in the cavity can be deduced from  $A_c(\lambda)$ , provided that the absorption cross-section is known and the relative density profile along the beam path can be estimated [11].

The majority of CRDS experiments have been made in the visible region of the spectrum, where very high quality mirrors are available (99.98% or better), allowing extremely weak absorbances to be observed (noise levels equivalent to linear absorption coefficients as low as  $10^{-10} \text{ cm}^{-1}$  have been reported). Unfortunately, relatively few molecules of interest have electronically-excited states that are low enough to be accessed from the ground state with a visible photon. Consequently, these studies have mostly focussed on vibrational overtone transitions of poly-atomic molecules. However, these forbidden transitions are extremely weak, so that the minimum concentrations that can be detected are rather high (corresponding to partial pressures of the

order of a Torr), despite the extremely high sensitivity in terms of absorbance.

Many more species can be excited to their first electronically excited state by near-UV photons (200–400 nm). However, the mirrors available in this region have relatively poor reflectivities. Nevertheless, with substantial signal averaging the equivalent single-pass noise level can be brought to as low as  $10^{-5}$  using commercially available mirrors with reflectivities of the order of 99.5%. This is largely adequate to detect low concentrations (down to  $10^{10} \text{ cm}^{-3}$ ) due to the large strengths of these transitions. Species (in most cases free radicals) that have been detected by near-UV CRDS include  $\text{CH}_3$  (216 nm [18]), OH (at 298 nm [19], 307 nm [20,21] and 248 nm [22]), Hg (253.7 nm [20]),  $\text{NH}_3$  (204.6 nm [20]), SH (307 nm [23]) and BrO (317 and 338 nm [24]).

When the spectral line-width of the injected laser is wider than that of the absorption feature in the cavity, the observed signal will show a multiple-, rather than single-, exponential decay. This is because, at any given laser central wavelength, only some of the laser modes will undergo absorption. This is often the case when an isolated rovibronic transition is probed, as the line-width of conventional pulsed dye lasers is broader than the room-temperature Doppler width of all but the lightest molecules. Zalicki and Zare [25] have investigated this effect by computer simulations. They concluded that the absolute species density can still be determined accurately from the CRDS signal, provided that: (1) the single-pass absorbance is not greater than the mirror losses; (2) the initial (fastest) decay rate is used; and (3) the absorbance is integrated over the line profile. The validity of this approach was subsequently confirmed by Newman et al. [26], who compared the intensities of CRDS and long-path FTIR absorption spectra of the a–X band of  $\text{O}_2$ .

## 2. Experimental

The experimental equipment is shown schematically in Fig. 1. The plasma reactor, which has been described previously [6], was somewhat modified in these experiments. It consists of an anodised aluminium reaction chamber (30 cm internal diameter by 4 cm high). The 11 cm diameter powered elec-

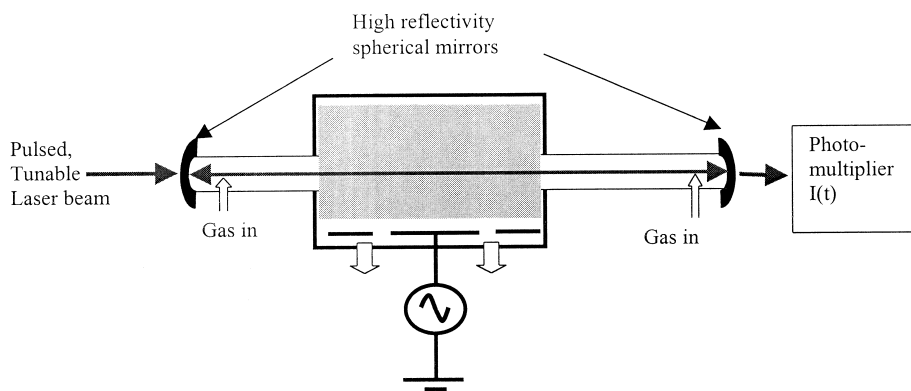


Fig. 1. Experimental apparatus.

trode is surrounded by a 27 cm external diameter coplanar earthed guard ring. The powered electrode was maintained at 20°C by cooling fluid in a closed-circuit thermostat. RF power (50–200 W) at 13.56 MHz was supplied by an L-type matching network.

The flow of feedstock gas ( $\text{CF}_4$  and  $\text{C}_2\text{F}_6$ ) was supplied to the reactor via a mass flow controller and evacuated with a throttled oil diffusion pump. The gas pressures used varied between 50 and 200 mTorr. The gas was injected close to the mirrors, which were mounted on 30 cm long 2 cm internal diameter tubes. In this way the gas flow served to limit the diffusion of reactive species to the mirror surfaces.

The optical ring-down cavity was comprised of spherical dielectric mirrors (1.5 m radius of curvature, mounted on flexible bellows with micrometric tilting mounts) separated by 1.00 m. The reflectivity of the mirrors was initially  $\sim 99.5\%$ , giving empty-cavity ring-down times of  $\sim 700$  ns, but this degraded to  $\sim 350$  ns after prolonged exposure to the plasma. The laser beam passes through the centre of the reactor, 2 cm distant from both the powered electrode and the grounded reactor roof.

The laser beam was produced by a XeCl excimer-pumped dye laser (Lambda Physik LPX210i and LPD3000) with frequency doubling, providing up to 1 mJ output in the range 220–240 nm with a pulse duration of  $\sim 20$  ns. According to the manufacturer, the frequency spectrum of the doubled output consists of  $\sim 20$  modes spread over 8 GHz and spaced by 400 MHz. The beam quality was improved by a spatial filter consisting of a 5 cm FL lens and a 50  $\mu\text{m}$  pinhole, re-collimated and injected

into the cavity with a 7 cm FL lens. This significantly improved the spectrum reproducibility and baseline stability.

The light exiting the opposite end of the cavity was detected with a photomultiplier tube (Hamamatsu R3896) fitted with a 225 nm interference filter to exclude visible light emitted by the plasma. The voltage divider was modified so that only 5 dynode stages were used. In this way the dynodes could be used with the correct voltage drop without drawing excessive current from the last stage. The amplified signal was digitised using a 1 GHz 8 bit sampling oscilloscope (but typically running at 4 ns/point) and transferred to a PC for analysis. The background signal level (taken before the laser shot) subtracted, and the exponential decay constant,  $k$  ( $=1/\tau$ ), determined from a linear fit to the logarithm of the data, using  $1/y$  weighting. The fit was generally performed using the data for 400 ns just after the end of the laser pulse. Typically, 10 laser shots were averaged for each spectral point, so that the laser wavelength could be scanned over  $1\text{ cm}^{-1}$  in 20 s using a 10 Hz repetition rate. The baseline signal (corresponding to the mirror losses) was subtracted from the signal, either by taking data with and without the plasma ignited at each point (for  $\text{CF}_2$ ), or by taking a whole spectrum with the plasma off.

### 3. Results

An example of the absorption spectra obtained is shown in Fig. 2. This shows the strong  $\text{A}^1\Pi \leftarrow$

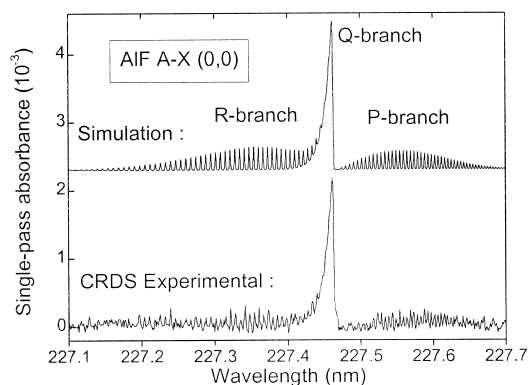


Fig. 2. CRDS spectrum of AIF in a  $\text{CF}_4$  plasma (50 mTorr, 150 W RF power), with no substrate on the Al powered electrode.

$X^1\Sigma^+$  transition of the AIF molecule, present in a 200 mT  $\text{CF}_4$  plasma at 150 W RF power (presumably produced by reactive sputtering of the aluminium surface of the powered electrode). Also shown is a simulated spectrum, obtained using the rotational constants given by Huber and Herzberg [27], and assuming a rotational temperature of 450 K (which gave the best fit). The prominent central feature (the Q-branch) consists of closely spaced rotational lines ( $0.12 \text{ cm}^{-1}$  spacing, compared to a Doppler width of  $0.10 \text{ cm}^{-1}$  FWHM at 450 K). A simulation using the Doppler width showed that the absorption is indeed a true continuum at the peak of this feature, so that there was no problem of non-exponential ring-down. In the short-wavelength tail of the Q-branch the lines become somewhat more widely spaced, but this effect should introduce little error in the integrated intensity as these lines have low intensity. The column density was therefore deduced from the integral of the Q-branch absorption [11], giving a value of  $1.5 \times 10^{10} \text{ cm}^{-2}$ . If one assumes that significant concentrations of this highly reactive species are only found close to the powered electrode, the absorbing path length can be estimated to be  $\sim 10 \text{ cm}$ , giving a concentration of only  $\sim 10^9 \text{ cm}^{-3}$ . This value is  $\sim 5$  times lower than that deduced from broad-band absorption spectroscopy under similar conditions [11]. However, this lower concentration can be attributed to the significant modifications that were made to the reactor since those experiments. In particular, the bare Al counter-electrode at 3.3 cm

from the powered electrode was replaced with a fully-anodised reactor roof at 4 cm, and the probing light beam position was moved from adjacent to the powered electrode to a position equidistant from both surfaces.

We estimate that the minimum concentration of AIF that could be detected by this technique is of the order of  $1 \times 10^8 \text{ cm}^{-3}$ . This extremely low value is a consequence of the very large oscillator strength of this transition, which is all concentrated into the narrow Q-branch, combined with the much higher resolution of CRDS compared to the broad-band technique.

When a silicon wafer is installed on the powered electrode, the production of AIF is stopped, and silicon fluoride etch products are produced instead. Fig. 3 shows part of the absorption spectrum of the  $\text{SiF}_2$  molecule, which has been shown to be a significant product of silicon etching under these conditions [6,11]. Once again, the absorption features are very wide, so that non-single-exponential behaviour does not occur. Indeed, the unresolved rotational structure of these transitions is so broad that the higher resolution of the laser technique does not lead to better sensitivity than the broad-band technique [11]. Therefore, the amplitude of the absorption observed by CRDS is comparable, indicating a concentration of the order of  $10^{12} \text{ cm}^{-3}$ .

Fig. 4 shows part of the A–X(1,0) transition of the CF molecule, observed in a 200 mTorr  $\text{CF}_4$  plasma at 150 W RF power, along with a simulation of the rotational structure. The  $P_{22}$  and  $P_{11}$  band-heads are also indicated. In this case isolated rovibronic transitions are observed, so attention must be paid to

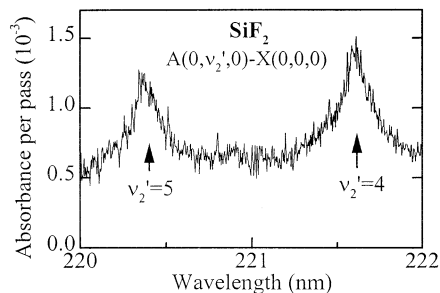


Fig. 3. CRDS spectrum of  $\text{SiF}_2$  in a  $\text{CF}_4$  plasma (50 mTorr 150 W RF power) with a Si substrate on the powered electrode.

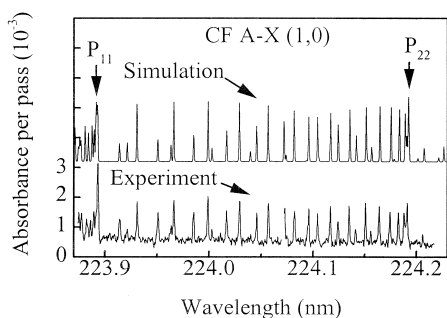


Fig. 4. CRDS spectrum of the CF A–X(1,0) band in a CF<sub>4</sub> plasma (200 mTorr, 150 W RF power).

non-single-exponential behaviour. However, as indicated by Zalicki and Zare [25], the concentration can be deduced with accuracy from the CRDS spectrum if only the initial part of the decay is used (as is the case here), and the spectrum is integrated over the band profile. The integral of the (1,0) band absorp-

tion was estimated by fitting the simulated spectrum, giving a value of the order of  $0.04 \text{ cm}^{-1}$ . This implies a CF concentration of  $6 \times 10^{11} \text{ cm}^{-3}$  in the reactor centre, a factor of 3 lower than that deduced previously from wide-band absorption. However, spatially-resolved LIF measurements [4] have shown that the concentration of CF decreases strongly as a function of distance from the powered electrode under these conditions. As the probe position used here is farther from the powered electrode than in the broad-band absorption experiments (2 cm from the electrode, compared to  $\sim 0.5$  cm), this lower value is not inconsistent with the previous results.

The A–X(0,0) band of CF was also observed at a wavelength of  $\sim 232.6$  nm, but this band is harder to analyse as it is confounded with the last weak bands of the A–X transition of the CF<sub>2</sub> molecule. Fig. 5 shows a more complete spectrum, this time of the CF A–X(2,0) band. This spectrum is of interest because the upper state is strongly pre-dissociated,

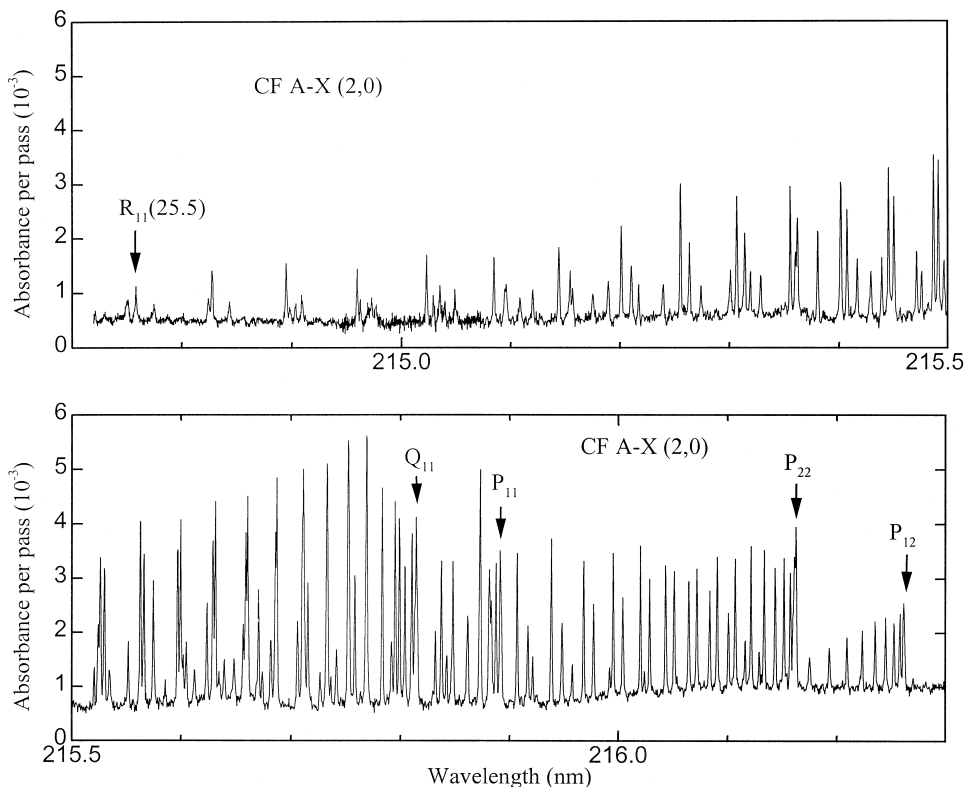


Fig. 5. CRDS spectrum of the CF A–X(2,0) band in a CF<sub>4</sub> plasma (200 mTorr, 150 W RF power). The upper state is pre-dissociated.

and therefore cannot be observed by emission spectroscopy [28], and only with great difficulty by LIF [29]. This is therefore the most complete spectrum of this transition published to date. Theoretical calculations indicate that the higher- $J$  lines should exhibit broadening due to lifetime-shortening [29]. However, the highest rotational line identified ( $J = 25.5$  in the figure) does not appear to be broadened. As the spectral resolution is of the order of 12 GHz, this indicates that the lifetime of this level is at least 13 ps. A theoretical estimate of the lifetime of this level gave a value of 1.2 ns [29], and suggested that the pre-dissociation broadening would only become comparable to the experimental line-width for  $J \approx 50$ .

Finally, an apparently chaotic but reproducible feature attributable to the  $\text{CF}_2$   $A-X(0, 10, 0) \leftarrow (0, 0, 0)$  band was observed at wavelengths around 237 nm. As the rotational constants of the A-state have only been deduced [30] for  $v_2'$  up to 5, we were unable to simulate the observed structure. However, with suitable mirrors it would be possible to access the  $(0, 5, 0) \leftarrow (0, 0, 0)$  band at 252 nm, which is both significantly stronger, and for which the spectroscopy is known.

#### 4. Conclusions

Laser cavity ring-down spectroscopy has been shown to be a powerful technique for detecting a wide range of reactive free radicals in reactive gas plasmas. With precautions, absolute concentrations can be deduced. When the majority of the transition strength is located in a spectrally narrow feature, as was the case for AIF, extremely low concentrations can be detected. For spectrally broad features there is less of an advantage over simpler broad-band absorption techniques. The technique offers the possibility of real-time (1 s resolution) absolute concentration measurements, provided that absorption is strong enough that any instability of the signal baseline is insignificant, allowing the concentration to be determined from the signal at the peak of a transition without wavelength scanning.

#### Acknowledgements

Jeff Steinfeld of MIT is thanked for providing the UV mirrors used for these experiments.

#### References

- [1] D.L. Flamm, V.M. Donnelly, *Plasma Chem. Plasma Proc.* 1 (1981) 317.
- [2] J.W. Coburn, *Plasma Chem. Plasma Proc.* 2 (1982) 1.
- [3] M.A. Lieberman, A.J. Lichtenberg, *Principles of Plasma Discharges and Materials Processing*, Wiley, New York, 1994.
- [4] J.P. Booth, G. Cunge, P. Chabert, N. Sadeghi, *J. Appl. Phys.* 85 (1999) 3097.
- [5] G. Cunge, J.P. Booth, *J. Appl. Phys.* 85 (1999) 3952.
- [6] G. Cunge, P. Chabert, J.P. Booth, *Plasma Sources, Sci. Technol.* 6 (1997) 349.
- [7] G. Cunge, J.P. Booth, J. Derouard, *Chem. Phys. Lett.* 263 (1996) 645.
- [8] K. Maruyama, A. Sakai, T. Goto, *J. Phys. D* 26 (1993) 199.
- [9] K. Maruyama, K. Ohkouchi, Y. Ohtsu, T. Goto, *Jpn. J. Appl. Phys.* 33 (1994) 4298.
- [10] M. Haverlag, E. Stoffels, W.W. Stoffels, G.M.W. Kroesen, F.J. de Hoog, *J. Vac. Sci. Technol. A* 14 (1996) 384.
- [11] J.P. Booth, G. Cunge, F. Neuilly, N. Sadeghi, *Plasma Sources, Sci. Technol.* 7 (1998) 423.
- [12] A. O'Keefe, D.A.G. Deacon, *Rev. Sci. Instrum.* 59 (1988) 2544.
- [13] M.D. Wheeler, S.M. Newman, A.J. Orr-Ewing, M.N.R. Ashfold, *J. Chem. Soc., Faraday Trans.* 94 (1998) 337.
- [14] D. Romanini, K.K. Lehmann, *J. Chem. Phys.* 99 (1993) 6287.
- [15] M. Kotterer, J. Conceicao, J.P. Maier, *Chem. Phys. Lett.* 259 (1996) 233.
- [16] A. Campargue, D. Romanini, N. Sadeghi, *J. Phys. D* 31 (1998) 1168.
- [17] D. Romanini, A.A. Kachanov, N. Sadeghi, F. Stoeckel, *Chem. Phys. Lett.* 264 (1997) 316.
- [18] P. Zalicki, Y. Ma, R.N. Zare, E.H. Wahl, J.R. Dadiamo, T.G. Owano, C.H. Kruger, *Chem. Phys. Lett.* 234 (1995) 269.
- [19] G. Meijer, G.H. Boogaarts, R.T. Jongma, D.H. Parker, *Chem. Phys. Lett.* 217 (1994) 112.
- [20] R.T. Jongma, M.G.H. Boogaarts, I. Holleman, G. Meijer, *Rev. Sci. Instrum.* 66 (1995) 2821.
- [21] S. Cheskis, I. Derzy, V.A. Lozovsky, A. Kachanov, D. Romanini, *Appl. Phys. B* 66 (1998) 377.
- [22] J.J.L. Spaanjaars, J.J. ter Muelen, G. Meijer, *J. Chem. Phys.* 107 (1997) 2242.
- [23] M.D. Wheeler, A.J. Orr-Ewing, M.N.R. Ashfold, T. Ishiwata, *Chem. Phys. Lett.* 268 (1997) 421.
- [24] M.D. Wheeler, S.M. Newman, T. Ishiwata, M. Kawasaki, A.J. Orr-Ewing, *Chem. Phys. Lett.* 285 (1998) 346.
- [25] P. Zalicki, R.N. Zare, *J. Chem. Phys.* 102 (1995) 2708.
- [26] S.M. Newman, I.C. Lane, A.J. Orr-Ewing, D.A. Newnham, J. Ballard, *J. Chem. Phys.* 110 (1999) 10749.
- [27] K.P. Huber, G. Herzberg, *Constants of Diatomic Molecules*, Van Nostrand Reinhold, New York, 1979.
- [28] T.L. Porter, D.E. Mann, N. Acquista, *J. Mol. Spectrosc.* 16 (1965) 228.
- [29] J.P. Booth, G. Hancock, M.J. Toogood, K.G. McKendrick, *J. Phys. Chem.* 100 (1996) 47.
- [30] C.W. Mathews, *Can. J. Phys.* 45 (1967) 2355.